nature neuroscience

Reduced sodium current in GABAergic interneurons in a mouse model of severe myoclonic epilepsy in infancy

Frank H Yu[1], Massimo Mantegazza[1,4], Ruth E Westenbroek[1], Carol A Robbins[2,3], Franck Kalume[1], Kimberly A Burton[1], William J Spain[3], G Stanley McKnight[1], Todd Scheuer[1] & William A Catterall[1]

Voltage-gated sodium channels (Na_V) are critical for initiation of action potentials. Heterozygous loss-of-function mutations in $Na_V1.1$ channels cause severe myoclonic epilepsy in infancy (SMEI). Homozygous null *Scn1a*$^{-/-}$ mice developed ataxia and died on postnatal day (P) 15 but could be sustained to P17.5 with manual feeding. Heterozygous *Scn1a*$^{+/-}$ mice had spontaneous seizures and sporadic deaths beginning after P21, with a notable dependence on genetic background. Loss of $Na_V1.1$ did not change voltage-dependent activation or inactivation of sodium channels in hippocampal neurons. The sodium current density was, however, substantially reduced in inhibitory interneurons of *Scn1a*$^{+/-}$ and *Scn1a*$^{-/-}$ mice but not in their excitatory pyramidal neurons. An immunocytochemical survey also showed a specific upregulation of $Na_V1.3$ channels in a subset of hippocampal interneurons. Our results indicate that reduced sodium currents in GABAergic inhibitory interneurons in *Scn1a*$^{+/-}$ heterozygotes may cause the hyperexcitability that leads to epilepsy in patients with SMEI.

Voltage-gated Na^+ channels in the brain are complexes of a 260-kDa α-subunit in association with auxiliary β-subunits (β1–β4) of 33 to 36 kDa[1,2]. The α-subunit contains the voltage sensors and the ion-conducting pore in four internally repeated domains (I–IV), each of which consists of six α-helical transmembrane segments (S1–S6) and a pore loop that connects S5 and S6 (ref. 1). The association of β-subunits modifies the kinetics and voltage dependence of gating, and these subunits are cell adhesion molecules that interact with the extracellular matrix, other cell adhesion molecules and the cytoskeleton[3,4]. The type I sodium channel, $Na_V1.1$, is the prototype of the voltage-gated sodium channel family in mammals[5]. $Na_V1.1$ is specifically localized in the neuronal cell body[6]; $Na_V1.2$ is localized in dendrites, unmyelinated axons and premyelinated axons[6–9]; and $Na_V1.6$ is localized in dendrites and in the nodes of Ranvier[8–10]. $Na_V1.3$ is abundant in the cell bodies of neurons during fetal and neonatal development but declines in adult rodents as the level of $Na_V1.1$ channels increases rapidly in the second postnatal week[11–13].

Voltage-gated sodium channels have crucial roles in the initiation and propagation of action potentials and are crucial regulators of neuronal excitability. Mutations in the $Na_V1.1$ channel gene, *SCN1A*, cause genetically distinct epilepsy syndromes. SMEI[14] is linked to *de novo* loss-of-function mutations in the *SCN1A* gene, which potentially lead to haploinsufficiency of $Na_V1.1$ channels[14–16]. This rare convulsive disorder begins during the first year of life, with seizures often associated with fever, and progresses to prolonged, clustered or continuous seizures and to *status epilepticus*[17,18]. After the second year of life, patients develop psychomotor delay, ataxia and cognitive impairment. They have an unfavorable long-term outcome because of the ineffectiveness of antiepileptic drug therapy[18,19].

It was a surprise that haploinsufficiency of a Na_V channel causes epilepsy, because reduced sodium current should lead to inexcitability rather than hyperexcitability. To generate an animal model for SMEI, we ablated the *Scn1a* gene in mouse. We report here that the null mutation of *Scn1a* leads to death on P15. In heterozygotes, which genetically mimic human SMEI, we describe an epileptic phenotype that has a striking strain-specific penetrance. A dramatic loss of sodium current in hippocampal GABAergic inhibitory interneurons in these mice may underlie their epilepsy. Upregulation of the expression of $Na_V1.3$ channels is insufficient to compensate. Our results point to a failure of excitability of hippocampal GABAergic inhibitory neurons as a possible cause for this intractable epilepsy syndrome.

RESULTS

Targeted disruption of the *Scn1a*

To disrupt the gene that encodes the $Na_V1.1$ channel, we used a replacement-type construct to target the last coding exon of *Scn1a*, which encodes domain IV downstream of the S3 segment and the cytoplasmic tail (**Fig. 1a**). Mouse lines were generated from two embryonic stem cell clones. Both had the expected deletion (**Fig. 1b** and data not shown) and showed the same phenotype. We bred the founding chimeric male to 129/SvJ females to generate congenic $Na_V1.1$-129Sv mice and to C57BL/6 for six generations to generate $Na_V1.1$-B6 mice. The three genotypes were born at expected Mendelian ratios in all heterozygous intercrosses, and mutants were indistinguishable from wild type in appearance and behavior until P9, which is

Departments of [1]Pharmacology, [2]Neurological Surgery and [3]Neurology, University of Washington, Seattle, Washington 98195-7280, USA. [4]Department of Neurophysiology, Instituto Neurologico Besta, via Temolo 4, 20126 Milano, Italy. Correspondence should be addressed to W.A.C. (wcatt@u.washington.edu).

Received 26 April; accepted 2 August; published online 20 August; corrected after print 13 December 2006; doi:10.1038/nn1754

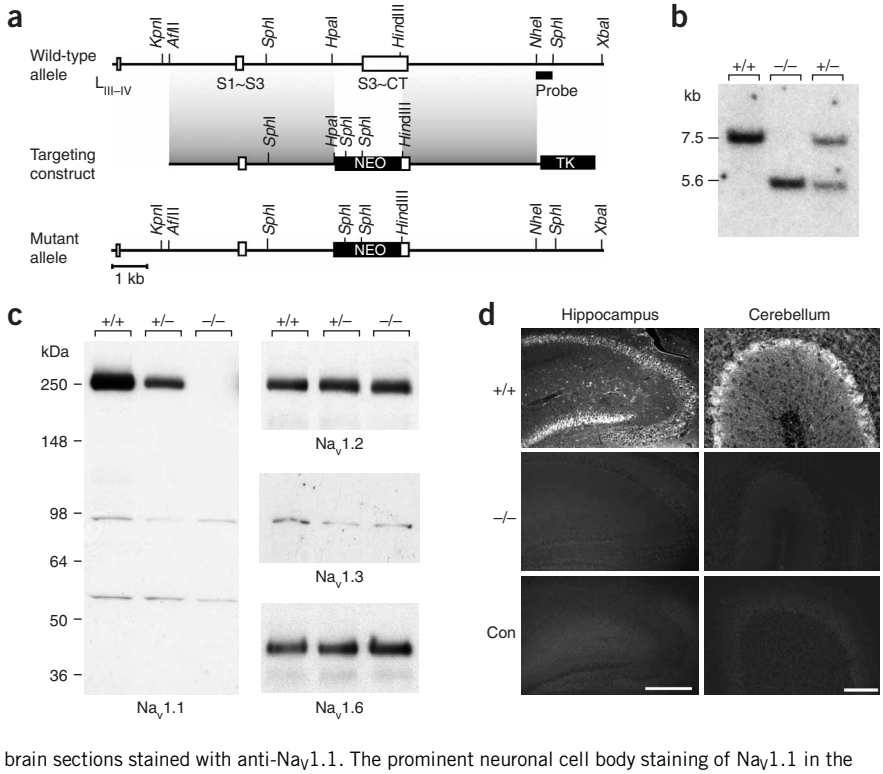

Figure 1 Targeting construct and generation of $Na_V1.1$ null mice. (**a**) Diagram of the targeting strategy used to ablate the $Na_V1.1$ channel. Homologous recombination of the targeting construct at the *Scn1a* gene locus results in the mutated allele in which most of the last coding exon is replaced by the neomycin-resistance gene cassette. The *Nhe*I/*Sph*I probe, localized 3′ externally to the targeting construct, recognizes a 7.5-kb fragment in *Sph*I-digested wild-type genomic DNA and a 5.6-kb fragment in the targeted genomic DNA because of the presence of *Sph*I restriction sites within the neomycin cassette. (**b**) Southern blot analysis of genomic DNA from offspring of a heterozygous intercross. An *Sph*I digest of genomic DNA was size fractionated, and the resulting Southern blot was probed with the *Nhe*I/*Sph*I probe. The presence of a 7.5-kb band indicates the wild-type allele, and a 5.6-kb band indicates the *Scn1a*-targeted allele. Genotypes are indicated by +/+ for wild type, +/– for heterozygous and –/– for homozygous. (**c**,**d**) Brain sodium channel expression in $Na_V1.1$ mutant mice. (**c**) Brain membrane proteins (100 μg) from wild-type and heterozygous and homozygous $Na_V1.1$ mice at P14 were analyzed by immunoblots using the indicated sodium channel–specific antibodies. Similar protein loading of wells is indicated by the nonspecific immunoreactive bands (55 and 95 kDa) of similar intensities in the left panel. (**d**) $Na_V1.1$ brain sections stained with anti-$Na_V1.1$. The prominent neuronal cell body staining of $Na_V1.1$ in the dentate gyrus, CA1-3 and the interneurons of the hippocampus (upper left panel) and the Purkinje cells of the cerebellum (upper right panel) of wild-type brains is completely absent in the homozygous *Scn1a*$^{-/-}$ brains (middle panels). The bottom panels (con) are no-primary antibody controls sectioned from wild-type brains. Scale bar: left panels, 200 μm; right panels, 100 μm.

consistent with the initial expression of $Na_V1.1$ channels in the second postnatal week[11–13]. Immunoblots with an antibody against the intracellular loop between domains I and II showed $Na_V1.1$ as a protein band of 250 kDa (**Fig. 1c**) whose intensity was reduced by approximately half in heterozygotes and was absent in homozygotes, which confirms that complete ablation of $Na_V1.1$ channels was achieved. There was no overall upregulation of $Na_V1.2$, $Na_V1.3$ or $Na_V1.6$ channels (**Fig. 1c**). As in previous studies, $Na_V1.1$ staining was restricted to the somata of central neurons, including pyramidal cells and inhibitory interneurons of the hippocampus and Purkinje neurons and granule neurons of the cerebellum (**Fig. 1d**; refs. 6,20). All staining was lost in *Scn1a*$^{-/-}$ mice (**Fig. 1d**).

Phenotype of homozygotes

$Na_V1.1$ null mice exhibited ataxia and seizures beginning on P9, leading progressively to mild limb tremors, side-to-side swaying and complete loss of postural control. By late P15, *Scn1a*$^{-/-}$ mice became inactive except for periodic generalized clonic and bilateral forelimb convulsive seizures. These mice did not survive beyond day 15, even when littermates were culled from the nursing dam (**Fig. 2a**,**b**). *Scn1a*$^{-/-}$ mice required significantly longer to recover from a supine to a prone position (**Fig. 2c**, $P < 0.05$), and they displayed a pronounced lack of coordination. Treatment with diazepam reduced the frequency of seizures, but all four mice given the drug died on P15. Postmortem examination showed no gross abnormalities except for the absence of stomach contents, lack of body fat and reduced weight. Hand-fed homozygous null mice survived as long as P17.5 (**Fig. 2d**) despite severe ataxia and seizures, which suggests that mice died of dehydration

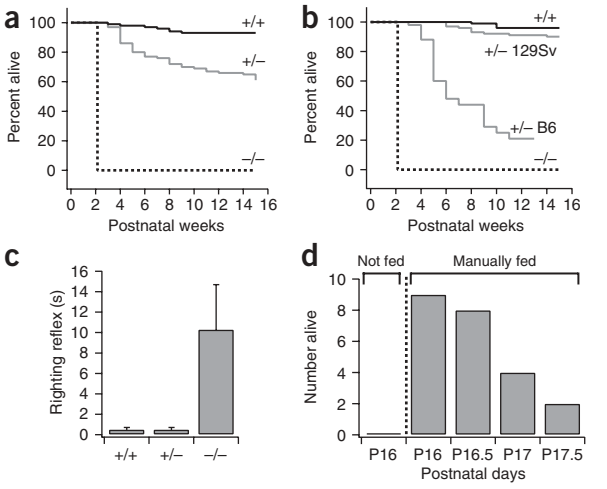

Figure 2 Premature deaths of $Na_V1.1$ mutant mice. (**a**) Survival plot of $Na_V1.1$ mutant mice in the hybrid 129SvJ:C57BL/6 genetic background, shown as the percentage of live mice at each postnatal week of age (wild type, $n = 233$; heterozygous, $n = 277$; homozygous, $n = 75$). (**b**) Survival plot of $Na_V1.1$ mutant mice in 129/SvJ and C57BL/6 genetic backgrounds, shown as the percentage of live mice at each postnatal week of age (wild type 129Sv, $n = 107$; homozygous 129Sv, $n = 34$; heterozygous 129Sv, $n = 111$; heterozygous B6, $n = 52$). (**c**) Righting reflex of $Na_V1.1$ mutant mice determined as latency in seconds to recover from a supine to prone position. Error bars are s.e.m. (**d**) Manual feeding can extend survival of $Na_V1.1$ knockout mice. Infant baby formula was gavaged directly into stomachs of $Na_V1.1$ null mice beginning on P14. One group ($n = 9$) was fed three or four times each day, and one group ($n = 4$) was not manually fed.

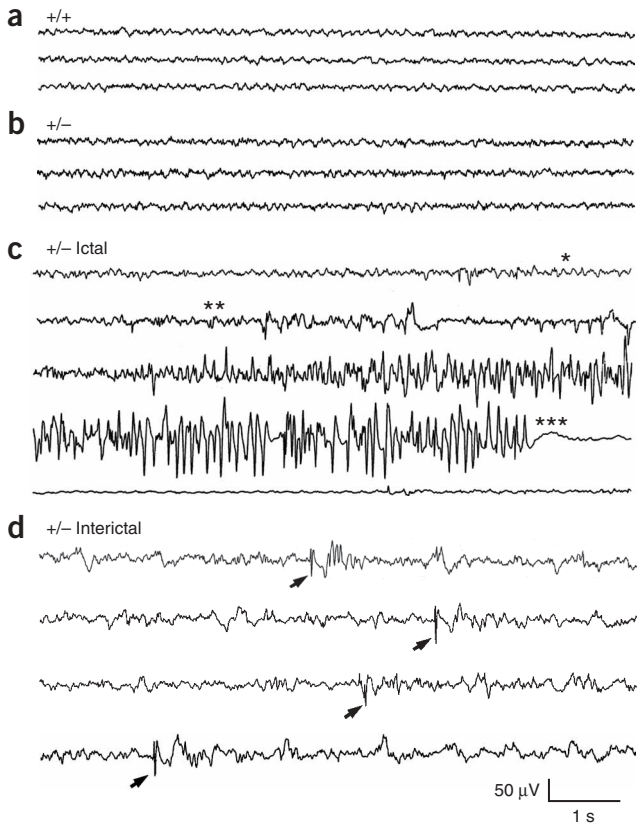

Figure 3 Spontaneous epileptic seizures in $Na_V1.1$ heterozygous mice. (**a**–**d**) Representative EEG recordings from a wild-type $Na_V1.1$(+/+) littermate (**a**) and from heterozygous *Scn1a*$^{+/-}$ mice during an interictal period without epileptiform activity (**b**), during an ictal episode (**c**) and during an interictal period with epileptiform activity (arrows; **d**). The recorded seizure began with a decrease in EEG voltage, followed by spiking activity that gradually increased in amplitude and rhythmicity and then ended with an isoelectric postictal period. Stereotypic seizure behavior: *Straub tail, myoclonic jerk, left hindlimb flexion; **bilateral forelimb clonus, head bobbing; ***relaxed muscle tone, end of seizure. Before the onset of behavioral seizure, each mouse was resting or sleeping and was fully recovered 30 s after seizure. Consecutive 8.4-s records from one EEG channel (left hemisphere) are shown; there was no difference in the spiking patterns between the left and right hemispheric activity in the examples shown.

and/or starvation that resulted from their inability to feed because of loss of motor control.

Phenotype of heterozygotes

Scn1a$^{+/-}$ mice first showed recurring behavioral seizures and sporadic deaths during the weaning period between P21 and P27. The seizures were spontaneous, and their frequency did not increase during routine handling (**Supplementary Video 1** online). Often $Na_V1.1$ heterozygous mice were found dead with outstretched hind limbs and front paws tucked under the chin, which is suggestive of death during an episode of *status epilepticus*. Survival plots (**Fig. 2a**) illustrate the incidence of sporadic death of 585 129/SvJ:C57BL/6 hybrid mice from F2 and F3 generations. All $Na_V1.1$ homozygous null mice died on P15. Many *Scn1a*$^{+/-}$ mice died during the third postnatal week, and approximately 40% of all heterozygous mice of both sexes died by the fifteenth week.

Spontaneous deaths were fourfold less (10% in 15 weeks) in the *Scn1a*$^{+/-}$ mice that were maintained in the 129/SvJ genetic background compared with the hybrid 129/SvJ:C57BL/6 background (**Fig. 2b**). In contrast, nearly 80% of heterozygous mice with the C57BL/6 background died by 13 weeks of age (**Fig. 2b**). No behavioral seizures were observed in heterozygous $Na_V1.1$-129Sv mice ($n \approx 150$), whereas they were frequent in heterozygous $Na_V1.1$-B6 mice. Evidently, the heterozygous phenotype of *Scn1a* ablation is much less penetrant in the 129/SvJ genetic background, even though the *Scn1a*$^{-/-}$ mice in this strain also died on P15. The surviving mutant mice in the C57BL/6 background showed impaired reproductive performance, which limited the number of heterozygotes available for experiments. In this work, we have thus analyzed the hybrid 129/SvJ:C57BL/6 mice.

EEG and spontaneous seizures

Some heterozygous mice with confirmed multiple behavioral seizures lived longer than 1 yr. To test for altered electroencephalographic activity, we recorded electroencephalogram (EEG) traces in freely moving 4-month-old mice during a 4-week period. Epileptiform activity was never observed either electrographically or behaviorally in wild-type mice ($n = 4$). Most EEG recording sessions with *Scn1a*$^{+/-}$

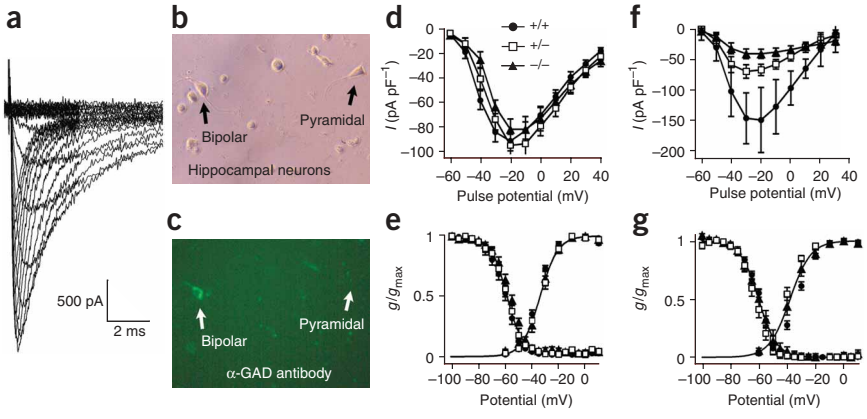

Figure 4 Sodium currents from hippocampal neurons in wild-type and heterozygous and null $Na_V1.1$ mice. (**a**) A representative set of sodium current traces from hippocampal pyramidal cells after subtraction of traces recorded in the presence of 1 μM tetrodotoxin, which were elicited by depolarizing steps from –60 to –15 mV in 5-mV increments from a holding potential of –100 mV. (**b**) Representative bright-field view of hippocampal neurons that were acutely dissociated from P14 wild-type mice. The pyramidal-shaped and bipolar-shaped neurons are indicated with arrows. (**c**) Same hippocampal neurons as in **b** but after immunocytochemical processing and staining with anti-GAD. The bipolar-shaped cells, but not the pyramidal-shaped cells, were strongly labeled, which indicates that they are GABAergic inhibitory interneurons. (**d**,**f**) Current density–voltage relationships of whole-cell sodium currents from hippocampal pyramidal (**d**) and bipolar (**f**) neurons for wild-type, heterozygous and homozygous mice. Currents of heterozygous and homozygous bipolar neurons were significantly smaller than those of wild-type neurons ($P < 0.05$). (**e**,**g**) Voltage dependence of activation (right curves) and steady-state inactivation (left curves) of sodium currents from hippocampal pyramidal (**e**) and bipolar (**g**) neurons. Same symbols for mouse genotypes as in **d**. Error bars are s.e.m.

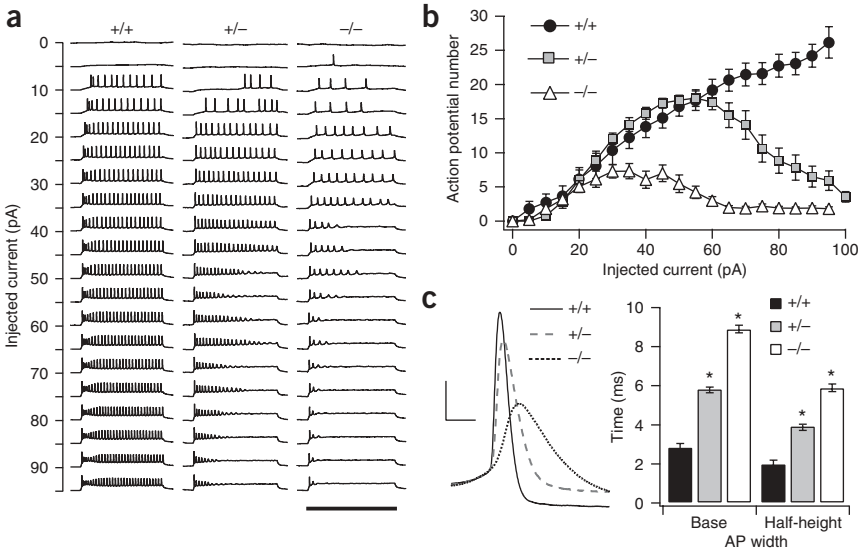

Figure 5 Depolarization-evoked firing activity of hippocampal interneurons from $Na_V1.1$ mutant mice. (**a**) Representative sets of action potential traces recorded from wild-type (+/+), heterozygous (+/–) and homozygous (–/–) interneurons during application of 800-ms injections of depolarizing current in +10-pA increments, from a holding potential of –80 mV. (**b**) Input-output relationship of the number of action potentials elicited versus the injected current. (**c**) Left panel, representative single action potentials recorded for each genotype of interneurons elicited by the same injected current amplitude (35 pA). Right panel, summary bar graph of action potential width and half-width, which are respectively defined as the width at the base and half-maximum amplitude of the action potential. Action potential parameters are listed in **Supplementary Table 1**. Error bars are s.e.m. $^*P < 0.01$.

heterozygotes showed normal periods of low-amplitude baseline cortical EEG activity (**Fig. 3a**,**b**). Video/EEG monitoring confirmed the occurrence of spontaneous electrographic and/or behavioral seizures (**Fig. 3c**), as well as epileptiform interictal activity (**Fig. 3d**), in three of seven $Na_V1.1$ heterozygous mice during the periods of continuous recording. Seizures began with stereotypic behaviors such as Straub tail, myoclonic jerks and hindlimb flexions, progressed to forelimb clonus and head bobbing and finished with relaxed muscle tone and an isoelectric period (**Fig. 3c**). The seizure duration was typically 20 s, and both clonic and tonic-clonic seizures were observed in these mutant mice.

Neuronal sodium currents

As epilepsy often involves hippocampal dysfunction, we dissociated neurons from mouse hippocampus and measured whole-cell sodium currents (**Fig. 4a**). We identified two populations of hippocampal neurons by morphology. Pyramidal-shaped cells were identified by their bulbous, triangular cell bodies with prominent proximal dendritic extensions, whereas interneuron-like cells were identified by their fusiform cell bodies with bipolar processes (**Fig. 4b**). Only the interneuron-like bipolar cells were specifically stained by an antibody to glutamic acid decarboxylase (anti-GAD; **Fig. 4c**), a key enzyme in the synthesis of GABA. These results verified our identification of these two populations of neurons based on morphology.

Whole-cell sodium currents recorded from wild-type, heterozygous and homozygous knockout pyramidal neurons were similar in current density (**Fig. 4d**), voltage dependence of activation (**Fig. 4e**) and voltage dependence of inactivation (**Fig. 4e**). In contrast, there was a substantial decrease in the sodium current levels of heterozygous and homozygous knockout interneurons. Our recordings yielded mean current densities of 149 ± 53 pA pF^{-1} for wild type, 70 ± 11 pA pF^{-1} for *Scn1a*$^{+/-}$ heterozygotes and 41 ± 8 pA pF^{-1} for *Scn1a*$^{-/-}$ homozygotes (**Fig. 4f**). Despite the large change in current amplitude, no changes in the voltage dependence of activation or inactivation of sodium currents were observed in interneurons (**Fig. 4g**). Approximately half of the sodium current was lost in heterozygous interneurons, but a smaller additional decrease was observed in homozygous interneurons. This nonlinear loss of sodium channels in interneurons suggests partial compensatory upregulation of another sodium channel in the homozygous knockout mice.

Neuronal firing pattern

The large reduction of sodium currents in interneurons from knockout mice should have significant effects on their firing properties. We recorded action potentials from dissociated hippocampal interneurons in response to a series of current injections and determined the input-output relationships (**Fig. 5a**). In wild-type interneurons, the number of action potentials increased nearly linearly with increasing depolarizing current over the range we examined (**Fig. 5b**). In contrast, the number of action potentials in interneurons from heterozygous and homozygous knockout mice reached a peak and declined with increasing injected current. The input-output plot showed a peak at 17 events in response to a 50-pA depolarizing current for *Scn1a*$^{+/-}$ interneurons, whereas the peak was observed at 7 events in response to a 35-pA depolarizing current for the *Scn1a*$^{-/-}$ interneurons (**Fig. 5b**). Notably, although no consistent changes were observed in input resistance or threshold for firing a single action potential, the amplitude of the action potential was significantly reduced and the width was substantially broadened in *Scn1a*$^{+/-}$ and *Scn1a*$^{-/-}$ mice (**Fig. 5c**; $P < 0.01$; **Supplementary Table 1** online). In addition, the peak of the action potential was greater, and the minimum voltage after the action potential was more negative in wild-type interneurons (action potential peak, 42.6 ± 2.2 mV; action potential minimum, −62.3 ± 5.4 mV; $n = 12$) compared with *Scn1a*$^{+/-}$

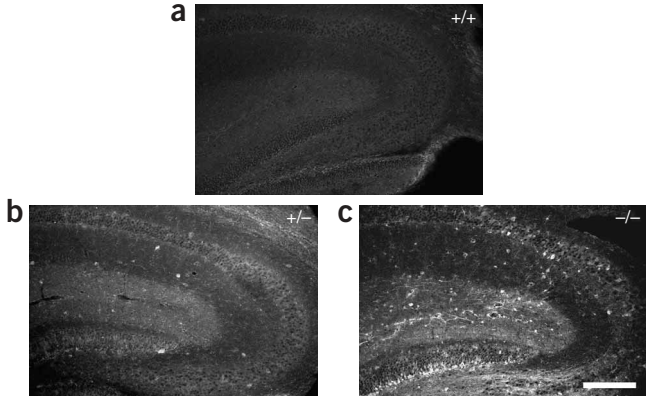

Figure 6 Upregulation of $Na_V1.3$ channels in the hippocampus of $Na_V1.1$ mutant mice. (**a**–**c**) Localization of $Na_V1.3$ channels by immunocytochemical staining with antibodies to $Na_V1.3$ in the hippocampus of wild-type (**a**) heterozygous (**b**) and homozygous (**c**) mice. Scale bar, 100 μm.

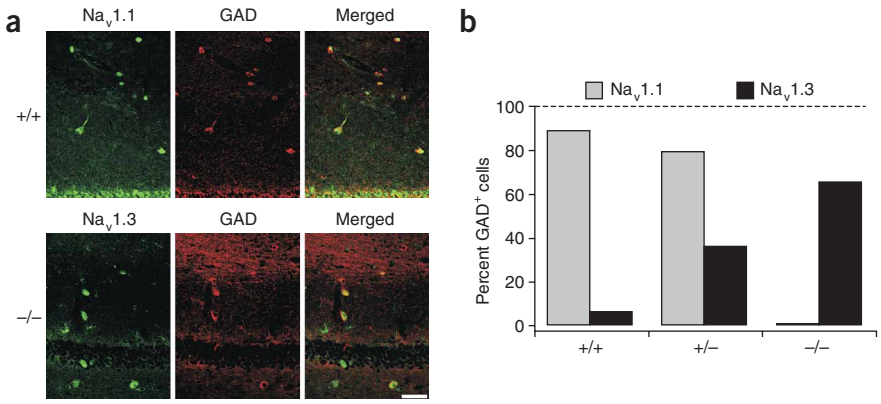

Figure 7 Upregulation of $Na_V1.3$ in GABAergic inhibitory interneurons. (**a**) Tissue sections of the CA1 region of hippocampus from a P14 wild-type (upper panels) or homozygous (lower panels) mouse were double-labeled with anti-$Na_V1.1$ or anti-$Na_V1.3$ and anti-GAD. Merged images illustrate the presence of the $Na_V1.1$ channel in most GAD-positive interneurons (yellow, upper-right panel) of wild-type hippocampus and show the upregulation of $Na_V1.3$ in the GAD-positive interneurons of homozygous hippocampus (lower-right panel). Scale bar, 100 μm. (**b**) Bar graph illustrating the percentage of GAD-positive interneurons in the hippocampus that were colabeled with either anti-Nav1.1 or anti-Nav1.3 in wild-type, heterozygous or knockout mice.

(action potential peak, 31.2 ± 5.3 mV; action potential minimum, –52.7 ± 3.3 mV; $n = 13$) or *Scn1a*$^{-/-}$ (action potential peak, 23.5 ± 3.0 mV; action potential minimum, –49.0 ± 3.0 mV; $n = 11$) interneurons. Overall, these data indicate that interneuron excitability and inhibitory control of downstream targets were substantially reduced in the hippocampus of mutant $Na_V1.1$ mice.

Compensatory upregulation of $Na_V1.3$ channels

Although our immunoblot analyses (**Fig. 1c**) showed no widespread upregulation of sodium channel subtypes, there could be substantial changes in sodium channel expression in specific brain regions. More extensive immunocytochemical analyses confirmed the loss of $Na_V1.1$ immunoreactivity throughout the brains of null mutant mice and no alteration in expression patterns of $Na_V1.2$ and $Na_V1.6$ (**Supplementary Note** and **Supplementary Figs. 1–5** online). Although there was no $Na_V1.3$ immunoreactivity in wild-type hippocampus (**Fig. 6a**), we were surprised to find an upregulation of $Na_V1.3$ in hippocampal interneurons of heterozygous and homozygous knockout mice at P14 (**Fig. 6b,c**). To identify GABAergic interneurons, we carried out double-labeling studies with anti-GAD, and we determined the percentage of interneurons that were positive for either $Na_V1.1$ or $Na_V1.3$ in the three genotypes of P14 mice. There were no changes in the number of GABAergic interneurons. We did, however, find that most GABAergic interneurons were stained for $Na_V1.1$ channels in wild-type mice and for $Na_V1.3$ channels in knockout mice (**Fig. 7a**). Of the GAD-positive interneurons, 89% (94/106) were positive for $Na_V1.1$ in wild-type mice versus 79.8% (83/104) in heterozygotes and 0% (0/100) in knockout mice (**Fig. 7b**). The opposite trend was observed for $Na_V1.3$ in GAD-positive cells: 5.7% (6/105) in wild type, 35.6% (36/101) in heterozygotes and 64.9% (63/97) in homozygous knockouts were double labeled. These findings indicate that most interneurons that were originally positive for $Na_V1.1$ in wild-type mice became immunoreactive for $Na_V1.3$ in the knockout mice, which demonstrates a compensatory upregulation that is specific to GABAergic inhibitory interneurons. This upregulation of $Na_V1.3$ channels is sufficient to compensate for only part of the loss of $Na_V1.1$ channels, however, as indicated by the sodium current recordings (**Fig. 4**). In addition, upregulation of $Na_V1.3$ channels was specific for hippocampal interneurons, as no upregulation was observed elsewhere in the brain (**Supplementary Figs. 1–5**).

DISCUSSION

$Na_V1.1$ channels are required for life

Our results show that the complete loss of $Na_V1.1$ is incompatible with brain function and leads to ataxia, seizures and ultimately premature death in the null mutant mice, apparently from a failure to feed because of ataxia and seizures. We did not expect this result, because $Na_V1.1$ channels are a minor component of total brain Na_V channels[12]. It is possible that the unique localization of $Na_V1.1$ channels in neuronal cell bodies[6] endows them with a crucial functional role in determining the level of electrical excitability of central neurons.

Epilepsy in $Na_V1.1$ heterozygotes

Haploinsufficiency of $Na_V1.1$ channels in heterozygous mutant mice leads to epileptic seizures in the fourth postnatal week. We were surprised to find that a reduction in Na_V channels leads to hyperexcitability. Nevertheless, this phenotype in mice phenocopies SMEI in humans in its severity, early age of onset and striking dependence on genetic background[18,21–24]. It is likely that the epileptic syndrome in *Scn1a*$^{+/-}$ mice has the same cellular and molecular basis as SMEI in humans, which would provide a unique model for the investigation of this disease.

Specific loss of sodium current in GABAergic interneurons

Our results show that sodium currents in GABAergic interneurons in the hippocampus of *Scn1a*$^{+/-}$ and *Scn1a*$^{-/-}$ mice are reduced much more substantially than are those in the pyramidal neurons. The pyramidal cells of the hippocampus express high amounts of $Na_V1.2$ and $Na_V1.6$ (refs. 6,25). Less than 10% of sodium channels in the hippocampus are $Na_V1.1$ channels, as determined by biochemical methods[12]. Our results indicate that at least 75% of the sodium current in GABAergic interneurons is conducted by $Na_V1.1$ channels. Therefore, $Na_V1.1$ channels must comprise less than 10% of the sodium channels in the pyramidal neurons. In agreement with this expectation, deletion of the Nav1.1 gene had no discernible effect on sodium currents in hippocampal pyramidal neurons. Because the standard error in our data from individual dissociated pyramidal cells was 10–15% (**Fig. 4d**), we could not detect a loss of $Na_V1.1$ channels if they contribute less than 10% of the total sodium current, as expected. In contrast to the pyramidal neurons, the 50% loss of sodium current in interneurons from heterozygotes indicates that $Na_V1.1$ channels may be responsible for most or all of the sodium current in these cells. The smaller further reduction in sodium current in the homozygous knockouts indicates that upregulation of $Na_V1.3$ channels may be much more prominent when $Na_V1.1$ channels are completely ablated and may partially compensate for their loss. The molecular basis for this upregulation and partial compensation is unknown, but it may involve a regulatory feedback loop between the amount of sodium current and the expression of sodium channels in interneurons, which is activated in *Scn1a*$^{-/-}$ mice.

Decreased excitability of GABAergic interneurons

The reduction of action potential number, frequency and amplitude in heterozygous and homozygous knockout interneurons that we observed in our current-clamp experiments illustrates their substantial impairment of excitability. As the threshold for the generation of single action potentials did not change after $Na_V1.1$ deletion, it is possible that $Na_V1.1$ channels may not have a major role in setting action potential threshold or, alternatively, that upregulation of $Na_V1.3$ channels may be sufficient for normal firing of single action potentials but not for sustained trains of action potentials. We postulate that the pronounced reduction in excitability of heterozygous and homozygous knockout interneurons in the hippocampus is an important factor that underlies the epileptic phenotype in mutant mice.

Sustained firing of GABAergic inhibitory interneurons is critical to the 'gate-keeper' function of the dentate gyrus in filtering neocortical and entorhinal excitatory inputs that converge into the CA3 region of the hippocampus[26–28]. GABAergic neuronal cell loss and reduced inhibition of granule cells in the dentate gyrus are associated with enhanced susceptibility to seizures in temporal lobe epilepsy[29–31]. Considering the importance of GABAergic interneurons in the control of excitability and in epileptic seizures, the specific reduction in the sodium current and in action potential firing in GABAergic interneurons that we have observed may be sufficient to cause epilepsy in our mouse model and in SMEI patients.

Upregulation of $Na_V1.3$ channels

In response to a loss of sodium current in interneurons, $Na_V1.3$ was upregulated in a subset of GABAergic inhibitory interneurons in the hippocampus of homozygous and heterozygous $Na_V1.1$ mutants at P14. Coexpression of $Na_V1.3$ channels and GAD was most clearly evident in the hilus and the subgranular region of the dentate gyrus. Evidently, the upregulation of $Na_V1.3$ channels occurs only in a subpopulation of GABAergic interneurons, as the number of double-positive cells for $Na_V1.3$ and GAD was substantially less in the $Na_V1.1$ null mice than was the number of double-positive $Na_V1.1$ and GAD cells in the wild type. Although our results show a steady increase in the number of interneurons that stained positively for $Na_V1.3$ (**Fig. 7**), immunocytochemical staining is not proportional to sodium channel density. Therefore, the increase in $Na_V1.3$ channel density may be much greater in the homozygous knockout mice. We observed a nonlinear decrease in total sodium current: 149 ± 53 pA pF^{-1} for wild type, 70 ± 11 pA pF^{-1} for *Scn1a*$^{+/-}$ and 41 ± 8 pA pF^{-1} for *Scn1a*$^{-/-}$ (**Fig. 4**). If there were no compensatory upregulation, these values should theoretically have been 149 pA pF^{-1}, 74.5 pA pF^{-1} and 0 pA pF^{-1}, respectively; that is, if deleting one *Scn1a* gene reduces the current by half, deleting the second *Scn1a* gene should reduce it to zero. In contrast to this expectation, our results indicate that $Na_V1.3$ conducts no current in the wild type because it is not expressed at detectable amounts (**Fig. 4b**), is upregulated (**Fig. 4b**) to not more than 11 pA pF^{-1} in heterozygotes (which would be undetectable given the cell-to-cell variability in our results), and is further upregulated such that it conducts up to 41 pA pF^{-1} in homozygous knockouts, which would account for most of the remaining sodium current in these cells. Although this upregulation would help to compensate for the loss of $Na_V1.1$ channels, our electrophysiological results show that these $Na_V1.3$ channels are not sufficient to restore normal amounts of sodium current, which leaves the GABAergic interneurons substantially deficient in excitability.

Genetic background effects

The heterozygous seizure phenotype was notably dependent on genetic factors beyond haploinsufficiency of $Na_V1.1$ channels, as 129/SvJ mice had no seizures and survived longer than did hybrid 129/SvJ:C57BL/6 mice, and C57BL/6 mice had more frequent seizures and died earlier. In contrast, the C57BL/6 mouse strain is more resistant than other strains to seizure induction by kainic acid[32], pentylenetetrazol[33], electroconvulsive shocks[34,35] and seizure-induced neuronal excitotoxicity[36,37]. Presumably, the genes that cause susceptibility to epilepsy in *Scn1a*$^{+/-}$ mice in the C57BL/6 background differ from those that cause resistance to seizures in these other experimental models. Because SMEI has a notably different onset and severity in different patients, these well-defined mouse lines provide a unique opportunity to identify susceptibility factors that influence SMEI and perhaps other forms of human epilepsy.

$Na_V1.1$ mutations in human epilepsy

Many mutations that alter the function of $Na_V1.1$ cause generalized epilepsy with febrile seizures plus ($GEFS^+$)[38,39]. SMEI is considered a severe form of $GEFS^+$ (ref. 22). Although different *SCN1A* mutations, including missense, nonsense, insertion, deletion and splice-donor site mutations, have been reported in SMEI, mutations that cause truncations predominate[21,40,41]. These genotype-phenotype correlation studies indicate that SMEI may typically be caused by loss-of-function *SCN1A* mutations that arise *de novo*, as the parents of these probands were not carriers of the defective allele[14,22,40]. SMEI patients have been recently described with *SCN1A* mutations that were, however, inherited from asymptomatic or mildly affected parents[23], which indicates that haploinsufficiency of the Nav1.1 channel by itself may not be sufficient to cause SMEI but may also require a permissive genetic setting[22,23]. The production of viable heterozygous $Na_V1.1$ mice with recurring seizures in our study provides clear evidence of heritability of the SMEI mutation, and our observation of variable penetration of the epileptic phenotype in different genetic backgrounds correlates with variable penetrance in humans and supports the notion that modifier gene(s) are necessary for SMEI. Candidates for genetic modifiers include genes that encode the GABA-A receptor β3 subunit, GABA-B receptor β1 subunit and glutamic acid decarboxylase 2 as well as the GABA-A receptor γ2 subunit, which are implicated in other inherited forms of epilepsy in mice and humans. Our recordings from hippocampal neurons indicate that deletion of $Na_V1.1$ may alter GABAergic output of inhibitory interneurons by decreasing their whole-cell sodium currents, without affecting sodium currents in excitatory pyramidal cells. Decreased sodium current in interneurons substantially decreases their ability for sustained action potential firing, which would reduce their GABAergic output and enhance the excitability of their downstream synaptic targets. Thus, our results connect the loss of $Na_V1.1$ channels in SMEI directly with the impairment of GABAergic neurotransmission in other forms of inherited epilepsy.

Therapy of SMEI

Patients with SMEI are refractory to therapy with the sodium channel–blocking anticonvulsant lamotrigine[42]. Resistance to lamotrigine is not surprising because it would be unexpected for a sodium channel blocker to be effective in a syndrome caused by haploinsufficiency of a sodium channel. The sodium channel blocker topiramate has, however, been found useful in SMEI patients[43] and has recently been recommended as a preferred chronic therapy in combination with valproate[44]. On the other hand, enhancement of GABAergic transmission by treatment with clonazepam or other benzodiazepines is a standard therapy for epilepsy and is effective in acute treatment of seizures in SMEI[44]. Our mouse model of SMEI may provide a useful test system to explore new approaches to both chronic and acute treatment of this intractable disease.

METHODS

Preparation of targeting construct and embryonic stem cell lines. A 15-kb 129/SvJ mouse *Scn1a* gene fragment that contains the terminal three coding exons in the λ DASH-II phage vector (a kind gift of P. Soriano, Fred Hutchinson Cancer Research Center and University of Washington) was assembled into the pNTK2 targeting vector[45] by subcloning a 3.6-kb short arm of the *Hin*dIII/*Nhe*I fragment and a 4.6-kb long arm of the *Hpa*I/*Afl*II fragment (**Fig. 1**), thereby replacing a large portion of the last coding exon with the neomycin gene for positive selection. The herpes simplex thymidine kinase gene was included in the vector for negative selection. The targeting construct was linearized at the *Not*I site in the polylinker and was electroporated into R1 embryonic stem cells[46] as described[47]. Embryonic stem cells were subjected to positive-negative selection using G418 (180 μg active/ml) and gancyclovir (200 μM), and double-resistant colonies were isolated on days 8 and 9 for expansion.

Mice. All animal care and use conformed to the National Institutes of Health Guide for Care and Use of Laboratory Mice and was approved by the University of Washington Institutional Animal Care and Use Committee.

Southern blot analysis and generation of mutant mice. Chromosomal DNA from embryonic stem cell clones was digested with *Sph*I and screened using Southern blot analysis with a 0.4-kb intronic probe spanning the *Nhe*I and *Sph*I sites immediately 3′ to the targeting construct. This probe hybridizes to 5.6-kb and 7.5-kb *Sph*I fragments of mutant and wild-type *Scn1a*, respectively. Two clones were selected for blastocyst-mediated transgenesis to generate male chimeras that were crossed to C57BL/6 females and 129/SvJ females and tested for germline transmission. The resulting heterozygous progeny were crossed to generate the mice used in this study.

Immunoblot analysis. Membranes were purified by discontinuous sucrose gradient centrifugation. Briefly, whole-brain lysates in 0.32 M sucrose/5 mM Tris, pH 7.4 were layered onto 1.2 M sucrose/5 mM Tris, pH 7.4 and centrifuged at 100,000*g* for 30 min. The protein fraction at the 0.8–1.2 M sucrose interface was collected, diluted twofold with 0.8 M sucrose/5 mM Tris, pH 7.4 and centrifuged at 20,000*g* for 20 min. Pelleted membrane proteins were resuspended in 1× RIA buffer (25 mM Tris, 150 mM NaCl, 1 mM EDTA, 2% Triton X-100, pH 7.4) and centrifuged at 20,000*g* for 20 min, and the supernatant containing the membrane proteins was collected for analysis. Complete Protease Inhibitor set (Roche) was included in all solutions. Membrane proteins (100 μg) were fractionated by SDS-PAGE and immunoblotted as described previously[48] using specific sodium channel antibodies: anti-$Na_V1.1$ (Chemicon; diluted 1:200), anti-$Na_V1.2$ (Chemicon, diluted 1:150), anti-$SP32_{III}$ ($Na_V1.3$; ref. 7; diluted 1:200), anti-SCN8a ($Na_V1.6$; Chemicon; diluted 1:150).

Immunocytochemistry. Tissue sections were prepared as described[49] and incubated in peptide affinity-purified primary anti-$Na_V1.1$ (diluted 1:20), anti-$Na_V1.3$ (Chemicon; diluted 1:20), anti-$Na_V1.2$ (diluted 1:20), anti-SP20 (ref. 6; diluted 1:20) or anti-SCN8a (Alomone; diluted 1:20) for 36 h at 4 °C. The sections were incubated in biotinylated goat anti–rabbit IgG, rinsed, washed as described[49] and viewed with a Bio-Rad MRC 600 microscope in the W.M. Keck Imaging Facility. For double-labeling experiments, monoclonal anti-GAD (Chemicon; diluted 1:200) was added at the same time as anti-$Na_V1.1$ or anti-$Na_V1.3$ and detected using anti–mouse IgG labeled with Texas red. For controls, the primary antiserum was omitted or replaced with normal rabbit serum.

Acutely dissociated hippocampal neurons (see below) were seeded onto polystyrene culture dishes, fixed in 4% paraformaldehyde for 20 min, rinsed and processed as described above for anti-GAD.

Electroencephalography. Under Ketamine/Xylazine anesthesia, chronic EEG electrodes were surgically implanted using aseptic technique in 10- to 12-week-old mice. Microscrews anchored into the cranium served as epidural electrodes and were connected to a microplug adhered to the cranium with dental acrylic. Recording electrodes were positioned bilaterally over each hemisphere (anterior-posterior, −2.0 mm from bregma; lateral, ±1.75 mm); a reference electrode was placed anterior to bregma (anterior-posterior, +0.5 mm) and a ground electrode was placed over the cerebellum. Mice were allowed to recover for 5–7 d before recording. The Telefactor Video/EEG Monitoring System was used to record EEGs and to videotape behavior simultaneously from unanesthetized free-moving mice. The low-frequency filter setting was 0.3 Hz, and the high-frequency filter was set at 70 Hz. Multiple sessions (three to six for each mouse) of 2- to 4-h recordings were obtained over a 4-week period.

Acute dissociation of hippocampal neurons. Hippocampal neurons were acutely isolated from P13 or P14 mice using standard procedures[50]. The cell suspension was placed in a 35-mm tissue culture dish mounted on the recording unit. After allowing the cells to settle for 5 min, the solution was changed to extracellular recording solution.

Electrophysiological recordings. Whole-cell patch-clamp recordings were carried out at room temperature using an Axopatch 200B amplifier (Axon Instruments) with PCLAMP 6 software (Axon Instruments) in voltage- or current-clamp configuration. For voltage-clamp experiments, cell capacitance (C_m) was calculated from $C_m = Q/V$, where Q is the charge measured by integrating the capacitative current evoked by a hyperpolarizing 10-mV voltage step (V) from a holding potential of –70 mV. For other recordings, capacitative currents were minimized using the amplifier circuitry. We routinely used 70% prediction and 90% series resistance compensation. The remaining linear capacity and leakage currents were eliminated by P/4 subtraction. The intracellular solution contained 177 mM *N*-methyl-D-glucamine, 40 mM HEPES, 4 mM $MgCl_2$, 10 mM EGTA, 1 mM NaCl, 25 mM phosphocreatine-Tris, 2 mM ATP-Tris, 0.2 mM Na_2GTP and 0.1 mM leupeptin, adjusted to pH 7.2 with H_2SO_4. The extracellular solution for the recording of peak Na^+ currents contained 20 mM NaCl, 116 mM glucose, 10 mM HEPES, 1 mM $BaCl_2$, 2 mM $MgCl_2$, 55 mM $CsCl_2$, 1 mM $CdCl_2$, 1 mM $CaCl_2$ and 20 mM tetraethylammonium chloride, adjusted to pH 7.35 with NaOH. Conductance-voltage (g-V) relationships (activation curves) were calculated according to $g = I_{Na}/(V - E_{Na})$, where I_{Na} is the peak Na^+ current measured at potential V, and E_{Na} is the calculated equilibrium potential. Normalized activation and inactivation curves were fit to Boltzmann relationships of the form $y = 1/(1 + \exp[(V - V_{1/2})/k]) + A$, where y is normalized g_{Na} or I_{Na}, A is the baseline conductance or current, V is the membrane potential, $V_{1/2}$ is the voltage of half-maximal activation (V_a) or inactivation (V_h) and k is a slope factor. In fitting the activation curves, A was fixed at 0. Analyses were carried out using Origin (Microcal) and pClamp (Axon Instruments).

For current-clamp experiments, cells were held at –80 mV, and their firing patterns were recorded in response to sustained depolarizations or hyperpolarizations (duration, 800 ms; increments, ±10 pA). The input-output relationship; action potential threshold, half-width, width and peak, minimum voltage; and input resistance of cells were measured. The input-output relationship was defined as the dependence of the number of action potentials generated upon the amplitude of current injection. The threshold was measured for the first action potential during the depolarization protocol as the voltage corresponding to the peak of the third differential of the action potential waveform. Action potential half-width and width were measured at half-height and threshold, respectively. Input resistance was determined as the slope of the linear regression of the I-V plot for a series of hyperpolarizing pulses, where I is current amplitude and V is steady-state voltage.

Grouped data are reported as mean ± s.e.m. Means and standard errors were compared using Student's t-test with $P < 0.05$ as the criterion for significance.

Note: Supplementary information is available on the Nature Neuroscience website.

ACKNOWLEDGMENTS

This work was supported by US National Institutes of Health Research Grants (W.A.C., T.S., G.S.M.), a Veteran's Administration Merit Review Grant (W.J.S), a grant from the McKnight Foundation (W.A.C.) and a Canadian Institutes of Health Research fellowship (F.H.Y.).

COMPETING INTERESTS STATEMENT

The authors declare that they have no competing financial interests.

Published online at http://www.nature.com/natureneuroscience
Reprints and permissions information is available online at http://npg.nature.com/reprintsandpermissions/

1. Catterall, W.A. From ionic currents to molecular mechanisms: the structure and function of voltage-gated sodium channels. *Neuron* **26**, 13–25 (2000).

2. Yu, F.H. & Catterall, W.A. Overview of the voltage-gated sodium channel family. *Genome Biol.* **4**, 207 (2003).
3. Isom, L.L. The role of sodium channels in cell adhesion. *Front. Biosci.* **7**, 12–23 (2002).
4. Isom, L.L. *et al.* Structure and function of the β2 subunit of brain sodium channels, a transmembrane glycoprotein with a CAM-motif. *Cell* **83**, 433–442 (1995).
5. Yu, F.H. & Catterall, W.A. The VGL-chanome: a protein superfamily specialized for electrical signaling and ionic homeostasis. *Sci. STKE* **2004**, re15 (2004).
6. Westenbroek, R.E., Merrick, D.K. & Catterall, W.A. Differential subcellular localization of the RI and RII Na^+ channel subtypes in central neurons. *Neuron* **3**, 695–704 (1989).
7. Westenbroek, R.E., Noebels, J.L. & Catterall, W.A. Elevated expression of type II Na^+ channels in hypomyelinated axons of shiverer mouse brain. *J. Neurosci.* **12**, 2259–2267 (1992).
8. Boiko, T. *et al.* Compact myelin dictates the differential targeting of two sodium channel isoforms in the same axon. *Neuron* **30**, 91–104 (2001).
9. Kaplan, M.R. *et al.* Differential control of clustering of the sodium channels $Na_V1.2$ and $Na_V1.6$ at developing CNS nodes of Ranvier. *Neuron* **30**, 105–119 (2001).
10. Caldwell, J.H., Schaller, K.L., Lasher, R.S., Peles, E. & Levinson, S.R. Sodium channel $Na_V1.6$ is localized at nodes of Ranvier, dendrites, and synapses. *Proc. Natl. Acad. Sci. USA* **97**, 5616–5620 (2000).
11. Beckh, S., Noda, M., Lübbert, H. & Numa, S. Differential regulation of three sodium channel messenger RNAs in the rat central nervous system during development. *EMBO J.* **8**, 3611–3616 (1989).
12. Gordon, D. *et al.* Tissue-specific expression of the RI and RII sodium channel subtypes. *Proc. Natl. Acad. Sci. USA* **84**, 8682–8686 (1987).
13. Scheinman, R.I. *et al.* Developmental regulation of sodium channel expression in the rat forebrain. *J. Biol. Chem.* **264**, 10660–10666 (1989).
14. Claes, L. *et al. De novo* mutations in the sodium-channel gene SCN1A cause severe myoclonic epilepsy of infancy. *Am. J. Hum. Genet.* **68**, 1327–1332 (2001).
15. Ohmori, I., Ouchida, M., Ohtsuka, Y., Oka, E. & Shimizu, K. Significant correlation of the SCN1A mutations and severe myoclonic epilepsy in infancy. *Biochem. Biophys. Res. Commun.* **295**, 17–23 (2002).
16. Fujiwara, T. *et al.* Mutations of sodium channel α subunit type 1 (*SCN1A*) in intractable childhood epilepsies with frequent generalized tonic-clonic seizures. *Brain* **126**, 531–546 (2003).
17. Engel, J., Jr. A proposed diagnostic scheme for people with epileptic seizures and with epilepsy: report of the ILAE task force on classification and terminology. *Epilepsia* **42**, 796–803 (2001).
18. Dravet, C., Bureau, M., Guerrini, R., Giraud, N. & Roger, J. Severe myoclonic epilepsy in infants. in *Epileptic Syndromes in Infancy, Childhood and Adolescence* (eds. Roger, J. *et al.*) 75–102 (John Libbey, London, 1992).
19. Oguni, H., Hayashi, K., Awaya, Y., Fukuyama, Y. & Osawa, M. Severe myoclonic epilepsy in infants–a review based on the Tokyo Women's Medical University series of 84 cases. *Brain Dev.* **23**, 736–748 (2001).
20. Gong, B., Rhodes, K.J., Bekele-Arcuri, Z. & Trimmer, J.S. Type I and type II Na^+ channel alpha-subunit polypeptides exhibit distinct spatial and temporal patterning, and association with auxiliary subunits in rat brain. *J. Comp. Neurol.* **412**, 342–352 (1999).
21. Claes, L. *et al. De novo* SCN1A mutations are a major cause of severe myoclonic epilepsy of infancy. *Hum. Mutat.* **21**, 615–621 (2003).
22. Singh, R. *et al.* Severe myoclonic epilepsy of infancy: extended spectrum of GEFS+? *Epilepsia* **42**, 837–844 (2001).
23. Nabbout, R. *et al.* Spectrum of SCN1A mutations in severe myoclonic epilepsy of infancy. *Neurology* **60**, 1961–1967 (2003).
24. Mulley, J.C. *et al.* SCN1A mutations and epilepsy. *Hum. Mutat.* **25**, 535–542 (2005).
25. Krzemien, D.M., Schaller, K.L., Levinson, S.R. & Caldwell, J.H. Immunolocalization of sodium channel isoform NaCh6 in the nervous system. *J. Comp. Neurol.* **420**, 70–83 (2000).
26. Lothman, E.W., Stringer, J.L. & Bertram, E.H. The dentate gyrus as a control point for seizures in the hippocampus and beyond. *Epilepsy Res. Suppl.* **7**, 301–313 (1992).
27. Schwartzkroin, P.A. Role of the hippocampus in epilepsy. *Hippocampus* **4**, 239–242 (1994).
28. Buhl, E.H., Halasy, K. & Somogyi, P. Diverse sources of hippocampal unitary inhibitory postsynaptic potentials and the number of synaptic release sites. *Nature* **368**, 823–828 (1994).
29. de Lanerolle, N.C., Kim, J.H., Robbins, R.J. & Spencer, D.D. Hippocampal interneuron loss and plasticity in human temporal lobe epilepsy. *Brain Res.* **495**, 387–395 (1989).
30. Buhl, E.H., Otis, T.S. & Mody, I. Zinc-induced collapse of augmented inhibition by GABA in a temporal lobe epilepsy model. *Science* **271**, 369–373 (1996).
31. Buckmaster, P.S. & Jongen-Relo, A.L. Highly specific neuron loss preserves lateral inhibitory circuits in the dentate gyrus of kainate-induced epileptic rats. *J. Neurosci.* **19**, 9519–9529 (1999).
32. Ferraro, T.N., Golden, G.T., Smith, G.G. & Berrettini, W.H. Differential susceptibility to seizures induced by systemic kainic acid treatment in mature DBA/2J and C57BL/6J mice. *Epilepsia* **36**, 301–307 (1995).
33. Ferraro, T.N. *et al.* Mapping loci for pentylenetetrazol-induced seizure susceptibility in mice. *J. Neurosci.* **19**, 6733–6739 (1999).
34. Ferraro, T.N. *et al.* Mouse strain variation in maximal electroshock seizure threshold. *Brain Res.* **936**, 82–86 (2002).
35. Frankel, W.N., Taylor, L., Beyer, B., Tempel, B.L. & White, H.S. Electroconvulsive thresholds of inbred mouse strains. *Genomics* **74**, 306–312 (2001).
36. Royle, S.J., Collins, F.C., Rupniak, H.T., Barnes, J.C. & Anderson, R. Behavioural analysis and susceptibility to CNS injury of four inbred strains of mice. *Brain Res.* **816**, 337–349 (1999).
37. Schauwecker, P.E. & Steward, O. Genetic determinants of susceptibility to excitotoxic cell death: implications for gene targeting approaches. *Proc. Natl. Acad. Sci. USA* **94**, 4103–4108 (1997).
38. Escayg, A. *et al.* A novel SCN1A mutation associated with generalized epilepsy with febrile seizures plus–and prevalence of variants in patients with epilepsy. *Am. J. Hum. Genet.* **68**, 866–873 (2001).
39. Wallace, R.H. *et al.* Neuronal sodium-channel alpha1-subunit mutations in generalized epilepsy with febrile seizures plus. *Am. J. Hum. Genet.* **68**, 859–865 (2001).
40. Sugawara, T. *et al.* Frequent mutations of SCN1A in severe myoclonic epilepsy in infancy. *Neurology* **58**, 1122–1124 (2002).
41. Fukuma, G. *et al.* Mutations of neuronal voltage-gated Na^+ channel alpha 1 subunit gene SCN1A in core severe myoclonic epilepsy in infancy (SMEI) and in borderline SMEI (SMEB). *Epilepsia* **45**, 140–148 (2004).
42. Guerrini, R. *et al.* Lamotrigine and seizure aggravation in severe myoclonic epilepsy. *Epilepsia* **39**, 508–512 (1998).
43. Coppola, G. *et al.* Topiramate as add-on drug in severe myoclonic epilepsy in infancy: an Italian multicenter open trial. *Epilepsy Res.* **49**, 45–48 (2002).
44. Ceulemans, B. *et al.* Severe myoclonic epilepsy in infancy: toward an optimal treatment. *J. Child Neurol.* **19**, 516–521 (2004).
45. Zhou, Q.Y., Quaife, C.J. & Palmiter, R.D. Targeted disruption of the tyrosine hydroxylase gene reveals that catecholamines are required for mouse fetal development. *Nature* **374**, 640–643 (1995).
46. Nagy, A., Rossant, J., Nagy, R., Abramow-Newerly, W. & Roder, J.C. Derivation of completely cell culture-derived mice from early-passage embryonic stem cells. *Proc. Natl. Acad. Sci. USA* **90**, 8424–8428 (1993).
47. Brandon, E.P., Gerhold, K.A., Qi, M., McKnight, G.S. & Idzerda, R.L. Derivation of novel embryonic stem cell lines and targeting of cyclic AMP-dependent protein kinase genes. *Recent Prog. Horm. Res.* **50**, 403–408 (1995).
48. Yu, F.H. *et al.* Sodium channel β4, a new disulfide-linked auxiliary subunit with similarity to β2. *J. Neurosci.* **23**, 7577–7585 (2003).
49. Westenbroek, R.E., Hoskins, L. & Catterall, W.A. Localization of Ca^{2+} channel subtypes on rat spinal motor neurons, interneurons, and nerve terminals. *J. Neurosci.* **18**, 6319–6330 (1998).
50. Cantrell, A.R., Ma, J.Y., Scheuer, T. & Catterall, W.A. Muscarinic modulation of sodium current by activation of protein kinase C in rat hippocampal neurons. *Neuron* **16**, 1019–1025 (1996).

nature neuroscience

Erratum: Reduced sodium current in GABAergic interneurons in a mouse model of severe myoclonic epilepsy in infancy

Frank H Yu, Massimo Mantegazza, Ruth E Westenbroek, Carol A Robbins, Franck Kalume, Kimberly A Burton, William J Spain, G Stanley McKnight, Todd Scheuer & William A Catterall

***Nature Neuroscience* 9, 1142–1149 (2006); published 20 August; corrected after print 13 December 2006**

In the version of this article initially published online, the acceptance date was incorrect. The paper was accepted on 2 August 2006. This error has been corrected in the PDF version of the article.

Corrigendum: Selective inhibition of 2-AG hydrolysis enhances endocannabinoid signaling in hippocampus

Judit K Makara, Marco Mor, Darren Fegley, Szilárd I Szabó, Satish Kathuria, Giuseppe Astarita, Andrea Duranti, Andrea Tontini, Giorgio Tarzia, Silvia Rivara, Tamás F Freund & Daniele Piomelli

Nature Neuroscience **8**, 1139–1141 (2005); **Published online 7 August 2005**

Our paper identified 6-methyl-2-*p*-tolylaminobenzo[*d*]oxazin-4-one (URB754; Specs) as a monoacylglycerol lipase (MGL) inhibitor that enhances hippocampal depolarization-induced suppression of inhibition (DSI). However, in subsequent tests of non-commercial URB754, we failed to replicate these results, suggesting that a bioactive impurity was present in the commercial material. We have identified this impurity as bis(methylthio)mercurane (**Supplementary Results** online). Because this compound interacts with multiple targets, we tested another MGL inhibitor, methylarachidonylfluorophosphonate (MAFP), which prolonged DSI (**Fig. 1**), confirming that monoacylglycerol lipase contributes to the termination of DSI, as others have reported[1]. Another generation of endocannabinoid metabolism inhibitors is needed to test this hypothesis further.

Note: Supplementary information is available on the Nature Neuroscience website.

1. Szabo B *et al. J. Physiol. (Lond.)* **577**, 263–280 (2006).

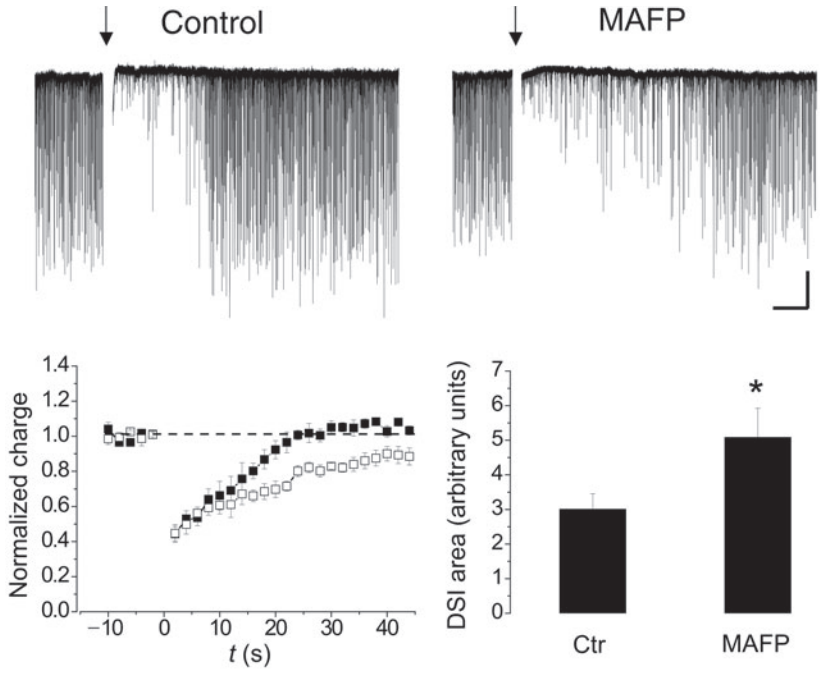

Figure 1 Effects of MAFP on DSI in hippocampal CA1 pyramidal cells. Top, traces from a representative experiment showing the effects of vehicle (ethanol, 0.00003%) or MAFP (Tocris, 45 nM) on the transient reduction of spontaneous inhibitory postsynaptic potentials (IPSCs) elicited by a depolarizing stimulus (arrow). Scale bars, 100 pA, 5 s. Bottom left, averaged time-course of DSI after administration of vehicle (solid squares) or MAFP (open squares). Bottom right, DSI area in the first 30 s after stimulus application was significantly larger in MAFP-treated than in control slices.

Erratum: Reduced sodium current in GABAergic interneurons in a mouse model of severe myoclonic epilepsy in infancy

Frank H Yu, Massimo Mantegazza, Ruth E Westenbroek, Carol A Robbins, Franck Kalume, Kimberly A Burton, William J Spain, G Stanley McKnight, Todd Scheuer & William A Catterall

Nature Neuroscience **9**, 1142–1149 (2006); **published online 20 August; corrected after print 13 December 2006**

In the version of this article initially published, the acceptance date was incorrect. The paper was accepted on 2 August 2006. This error has been corrected in the PDF versions of the article.

Erratum: The many roots of aggression

Jordan Grafman, Maren Strezniak & Frank Krueger

Nature Neuroscience **9**, 1347 (2006); **published online 26 October 2006; corrected after print 21 November 2006**

In the version of this article initially published, the second author's name was spelled incorrectly. The correct name should be Maren Strenziok. The error has been corrected in the HTML and PDF versions of the article.